

A Steam Generator Water Level Controller Using a Receding Horizon Control Method

Man Gyun Na

Chosun University
375 Seosuk-dong, Dong-gu, Kwangju 501-759, Republic of Korea

Yoon Joon Lee

Cheju National University
1 Ara 1-Dong, Cheju City, Cheju-Do 690-756, Republic of Korea

Abstract

In this work, this receding horizon control method was used to control the water level of nuclear steam generators and applied to a linear model and also a nonlinear model of steam generators. A receding horizon control method is to solve an optimization problem for finite future steps at current time and to implement the first optimal control input as the current control input. The procedure is then repeated at each subsequent instant. The dynamics of steam generators are very different according to power levels. The receding horizon controller was designed by using a reduced linear steam generator model fixed over a certain power range. The proposed controller designed at a fixed power level showed good performance for any other power level within this power range. The steam generator shows actually nonlinear characteristics. Therefore, the proposed algorithm was implemented for a nonlinear model of the nuclear steam generator to verify its real performance and also, showed good responses.

1. Introduction

To properly control the water level of a nuclear steam generator is very important in securing the sufficient cooling water of the nuclear reactor and in preventing the damage of turbine blades. The inadequate and insufficient performance of the conventional controller has often resulted in reactor trip (shutdown) and enforced operators to hang on manual operation at low power (mainly, at a startup time of a nuclear power plant). In particular, since the swell and shrink phenomena are significantly greater at low power, even to a skilled operator, it is hard to react effectively in response to such a reverse dynamics of the water level, which is induced by the non-minimum phase effects. Also, the steam generator is a highly complex, non-linear, and time-varying system. And its parameters undergo large changes according to changes in operating conditions [1]. The steam generator with narrow stability margin cannot work satisfactorily with fixed P-I gains over all power levels. Therefore, many advanced control methods that include adaptive controllers [1,2], optimal controllers [3,4], and fuzzy logic controllers [5-8], have been suggested to resolve the steam generator water level control problem.

The receding horizon control methodology has received much attention as a powerful tool for the control of industrial process systems [9-14]. The basic concept of the receding horizon control is to solve an optimization problem for a finite future at current time and to implement the first optimal control input as the current control input. The optimization solutions for a specified objective function and also manipulated variables for implementation are shown in Fig. 1 as time goes on. As it were, at the present time k , the present and future control inputs on the control horizon M , $u(k), u(k+1), \dots, u(k+M-1)$, and the predicted outputs over the prediction horizon N , $y(k+1), y(k+2), \dots, y(k+N)$, are obtained by solving an optimization problem represented by a specified objective function. Among these solutions, only the first computed change in the manipulated variable, $u(k)$, is implemented for time $[k, k+1]$. The procedure is then repeated at each subsequent instant. This method presents many advantages over the conventional infinite horizon control because it is possible to handle input and state (or output) constraints in a systematic manner during the design and implementation of the control. In particular, it is a suitable control strategy for time varying systems.

Therefore, in this work, the receding horizon control method was used to solve the steam generator water level control problems. The objective of this work is to design an automatic receding horizon controller which eliminates any manual operation from start-up to full load transient conditions. The proposed controller was applied to two different linear models [1,15] and also, to a nonlinear model [16] of the nuclear steam generator to

verify its real performance. The receding horizon controller was designed by using a reduced linear steam generator model fixed over a certain power range.

2. Receding Horizon Control Method

Receding horizon control is a popular technique for the control of slow dynamical systems. At every time instant receding horizon control requires the on-line solution of an optimization problem to compute optimal control inputs over a fixed number of future time instants, known as the time horizon. The on-line optimization can be typically reduced to either a linear program or a quadratic program.

The receding horizon control method is to solve an optimization problem for a finite future at current time and to implement the first optimal control input as the current control input. The procedure is then repeated at each subsequent instant. Figure 2 shows this basic concept [11]. As it were, for any assumed set of present and future control moves, the future behavior of the process outputs can be predicted over a horizon N , and the M present and future control moves ($M \leq N$) are computed to minimize a quadratic objective function. Though M control moves are calculated, only the first control move is implemented. At the next period, new values of the measured output are obtained, the control horizon is shifted forward by one step, and the same calculations are repeated.

The dynamics of a steam generator is described in terms of input (feedwater flowrate; u), output (water level; y) and measurable disturbance (steam flowrate; v). Based on the step response of the steam generator water level for step changes of the feedwater flowrate and the steam flowrate, Irving [1] derived the following 4-th order Laplace transfer function for steam generators:

$$Y(s) = \frac{G_1}{s} [U(s) - V(s)] - \frac{G_2}{1 + \tau_2 s} [U(s) - V(s)] + \frac{G_3 s}{\tau_1^{-2} + 4\pi^2 T^{-2} + 2\tau_1^{-1} s + s^2} U(s), \quad (1)$$

where

the capital letters, $Y(s)$, $U(s)$ and $V(s)$, represent the Laplace-transformed variables of the steam generator water level $y(t)$, the feedwater flowrate $u(t)$ and the steam flowrate $v(t)$, respectively,

τ_1 and τ_2 are damping time constants,

T is the period of the mechanical oscillation,

G_1 is the magnitude of the mass capacity effect,

G_2 is the magnitude of the swell or shrink due to the feedwater or steam flowrates,

G_3 is the magnitude of the mechanical oscillation.

The first term means the water level quantity due to the actual water inventory change induced by the feedwater inlet into the steam generator and the steam outlet from it. The second term means the water level quantity due to the swell and shrink phenomena which appear initially if the feedwater or steam flowrate changes and are opposite to long term effects. The last term means the water level quantity due to the mechanical oscillation. This is due to the momentum of the water in the downcomer keeping the recirculating flow going down initially and then slowing down, which causes the damping oscillations. The third term of the right hand side in Eq. (1) is extremely small in affecting the water level response [17]. Therefore, the 4-th order linear model can be reduced well without making a great difference to a second order linear model and the proposed control method can be designed by using this reduced nuclear steam generator model. If we neglect the third term in Eq. (1), nuclear steam generators can be described in the following discrete state equation:

$$\begin{aligned} \mathbf{x}(k+1) &= \mathbf{A}\mathbf{x}(k) + \mathbf{B}(\Delta u(k) - \Delta v(k)), \\ y(k) &= \mathbf{C}\mathbf{x}(k), \end{aligned} \quad (2)$$

where $\mathbf{x}(k) \in R^n$, $\Delta u(k) = u(k) - u(k-1)$, $\Delta v(k) = v(k) - v(k-1)$, and $y(k)$ are the state vector, control input (feedwater flowrate), measurable disturbance (steam flowrate), and process output (steam generator water level), respectively. In Eq. (2), the change of signals, Δu and Δv , was used to remove the offset error. From now on, to design the receding horizon controller, the following time invariant discrete system will be considered:

$$\begin{aligned} \mathbf{x}(k+1) &= \mathbf{A}\mathbf{x}(k) + \mathbf{B}\Delta u_{uv}(k), \\ y(k) &= \mathbf{C}\mathbf{x}(k), \end{aligned} \quad (3)$$

where

$$\Delta u_{uv}(k) = \Delta u(k) - \Delta v(k).$$

The associated performance index for designing the controller can be written as the following quadratic function:

$$J = \frac{1}{2} \sum_{j=0}^{N-1} \left[Q(\mathbf{C}\mathbf{x}(k+j) - r(k+j))^2 + \mu \Delta u_{uv}(k+j)^2 \right] + \frac{1}{2} Q_F (\mathbf{C}\mathbf{x}(k+N) - r(k+N))^2, \quad (4)$$

where r is a reference input (target water level), and Q (≥ 0), Q_F (≥ 0) and μ (> 0) are weighting values to penalize particular components of $(y - r)$ or Δu_{uv} at certain future time intervals. In the above equation, it is assumed that $\Delta u_{uv}(k+M) = \Delta u_{uv}(k+N) = 0$.

The objective is to find the control sequence, $u_{uv}(k), u_{uv}(k+1), \dots, u_{uv}(k+M-1)$, to minimize the quadratic function. In this work, the powerful Lagrange-multiplier approach will be used to derive a receding horizon controller for minimizing the above cost function. Since there is a constraint function $\mathbf{x}(k+1) = \mathbf{A}\mathbf{x}(k) + \mathbf{B}\Delta u_{uv}(k)$ or $\mathbf{x}(k+1) = \mathbf{A}\mathbf{x}(k)$ (note that $\Delta u_{uv}(k+M) = \Delta u_{uv}(k+N) = 0$) specified at each time k in the interval of interest $[k, k+N]$, we shall require a Lagrange multiplier at each time. We append the constraint to the performance index to define an augmented performance index J' by

$$J' = \sum_{j=0}^{M-1} \left[L_1^j(\mathbf{x}(k+j), \Delta u_{uv}(k+j)) + \boldsymbol{\lambda}(k+j+1)^T (\mathbf{A}\mathbf{x}(k+j) + \mathbf{B}\Delta u_{uv}(k+j) - \mathbf{x}(k+j+1)) \right] \\ + \sum_{j=M}^{N-1} \left[L_2^j(\mathbf{x}(k+j)) + \boldsymbol{\lambda}(k+j+1)^T (\mathbf{A}\mathbf{x}(k+j) - \mathbf{x}(k+j+1)) \right] + L_2^N(\mathbf{x}(k+N)), \quad (5)$$

where

$$L_1^j(\mathbf{x}(k+j), \Delta u_{uv}(k+j)) = \frac{1}{2} Q(\mathbf{C}\mathbf{x}(k+j) - r(k+j))^2 + \frac{1}{2} \mu \Delta u_{uv}(k+j)^2 \text{ for } j=0, \Lambda, M-1, \\ L_2^j(\mathbf{x}(k+j)) = \begin{cases} \frac{1}{2} Q(\mathbf{C}\mathbf{x}(k+j) - r(k+j))^2 & \text{for } j=M, \Lambda, N-1, \\ \frac{1}{2} Q_F(\mathbf{C}\mathbf{x}(k+j) - r(k+j))^2 & \text{for } j=N. \end{cases}$$

Defining the Hamiltonian function as

$$H^j(\mathbf{x}(k+j), \Delta u_{uv}(k+j), \boldsymbol{\lambda}(k+j+1)) \\ = \begin{cases} L_1^j(\mathbf{x}(k+j), \Delta u_{uv}(k+j)) + \boldsymbol{\lambda}(k+j+1)^T (\mathbf{A}\mathbf{x}(k+j) + \mathbf{B}\Delta u_{uv}(k+j)) & \text{for } j=0, \Lambda, M-1, \\ L_2^j(\mathbf{x}(k+j)) + \boldsymbol{\lambda}(k+j+1)^T (\mathbf{A}\mathbf{x}(k+j)) & \text{for } j=M, \Lambda, N-1, \end{cases} \quad (6)$$

we can rewrite the augmented performance index as follows:

$$J' = L_2^N(\mathbf{x}(k+N)) - \boldsymbol{\lambda}(k+N)^T \mathbf{x}(k+N) + H^0(\mathbf{x}(k), \Delta u_{uv}(k), \boldsymbol{\lambda}(k+1)) \\ + \sum_{j=1}^{N-1} \left[H^j(\mathbf{x}(k+j), \Delta u_{uv}(k+j), \boldsymbol{\lambda}(k+j+1)) - \boldsymbol{\lambda}(k+j)^T \mathbf{x}(k+j) \right]. \quad (7)$$

We now examine the increment in J' due to increments in all the variables, $\mathbf{x}(k+j)$, $\Delta u_{uv}(k+j)$, and $\boldsymbol{\lambda}(k+j)$. According to the Lagrange-multiplier theory, at a constrained minimum this increment dJ' should be zero. Therefore,

$$dJ' = \left(L_2^N_{\mathbf{x}(k+N)} - \boldsymbol{\lambda}(k+N) \right)^T d\mathbf{x}(k+N) + \left(H_{\mathbf{x}(k)}^0 \right)^T d\mathbf{x}(k) + H_{u_{uv}(k)}^0 du_{uv}(k) \\ + \sum_{j=1}^{N-1} \left[\left(H_{\mathbf{x}(k+j)}^j - \boldsymbol{\lambda}(k+j) \right)^T d\mathbf{x}(k+j) + H_{u_{uv}(k+j)}^j du_{uv}(k+j) \right] \\ + \sum_{j=1}^N \left(H_{\boldsymbol{\lambda}(k+j)}^{j-1} - \mathbf{x}(k+j) \right)^T d\boldsymbol{\lambda}(k+j), \quad (8)$$

where $H_{\mathbf{x}(k+j)}^j$ represents the differential of H^j with respect to $\mathbf{x}(k+j)$ such as $H_{\mathbf{x}(k+j)}^j \equiv \frac{\partial H^j}{\partial \mathbf{x}(k+j)}$ and so on.

Necessary conditions for a constrained minimum are thus given by

$$\mathbf{x}(k+j+1) = \frac{\partial H^j}{\partial \boldsymbol{\lambda}(k+j+1)}, \quad j=0, \Lambda, N-1, \quad (9)$$

$$\boldsymbol{\lambda}(k+j) = \frac{\partial H^j}{\partial \mathbf{x}(k+j)}, \quad j=1, \Lambda, N-1, \quad (10)$$

$$0 = \frac{\partial H^j}{\partial u_{uv}(k+j)}, \quad j=0, \Lambda, M-1, \quad (11)$$

which arise from the terms inside the summations of Eq. (8) and the coefficients of $du_{uv}(k)$, and

$$\left(\frac{\partial L_2^N}{\partial \mathbf{x}(k+N)} - \boldsymbol{\lambda}(k+N) \right)^T d\mathbf{x}(k+N) = 0, \quad (12)$$

$$\left(\frac{\partial H^0}{\partial \mathbf{x}(k)} \right)^T d\mathbf{x}(k) = 0. \quad (13)$$

From Eqs. (9)-(11)

$$\mathbf{x}(k+j+1) = \begin{cases} \mathbf{A}\mathbf{x}(k+j) + \mathbf{B}\Delta u_{uv}(k+j) & \text{for } j=0, \Lambda, M-1, \\ \mathbf{A}\mathbf{x}(k+j) & \text{for } j=M, \Lambda, N-1, \end{cases} \quad (14)$$

$$\boldsymbol{\lambda}(k+j) = \mathbf{C}^T \mathbf{Q} \mathbf{C} \mathbf{x}(k+j) + \mathbf{A}^T \boldsymbol{\lambda}(k+j+1) - \mathbf{C}^T \mathbf{Q} r(k+j), \quad \text{for } j=1, \Lambda, N-1, \quad (15)$$

$$0 = \mathbf{B}^T \boldsymbol{\lambda}(k+j+1) + \mu \Delta u_{uv}(k+j) \quad \text{for } j=0, \Lambda, M-1. \quad (16)$$

From Eq. (12), Boundary conditions are as follows:

$$\boldsymbol{\lambda}(k+N) = \mathbf{C}^T \mathbf{Q}_F (\mathbf{C} \mathbf{x}(k+N) - r(k+N)). \quad (17)$$

The stationarity condition, Eq. (16), shows that

$$\Delta u_{uv}(k+j) = -\mu^{-1} \mathbf{B}^T \boldsymbol{\lambda}(k+j+1). \quad (18)$$

The Lagrange multiplier is a variable that is determined by its own dynamical equation. It is called the costate of the system or the adjoint system. The coupled state and costate equations can be written as

$$\begin{bmatrix} \mathbf{x}(k+j+1) \\ \boldsymbol{\lambda}(k+j) \end{bmatrix} = \begin{bmatrix} \mathbf{A} & -\mathbf{B}\mu^{-1}\mathbf{B}^T \\ \mathbf{C}^T \mathbf{Q} \mathbf{C} & \mathbf{A}^T \end{bmatrix} \begin{bmatrix} \mathbf{x}(k+j) \\ \boldsymbol{\lambda}(k+j+1) \end{bmatrix} + \begin{bmatrix} \mathbf{0} \\ -\mathbf{C}^T \mathbf{Q} \end{bmatrix} r(k+j), \quad \begin{matrix} \text{for } j=0, \Lambda, M-1 \text{ (for } \mathbf{x}) \\ \text{for } j=1, \Lambda, M-1 \text{ (for } \boldsymbol{\lambda}) \end{matrix} \quad (19)$$

$$\begin{bmatrix} \mathbf{x}(k+j+1) \\ \boldsymbol{\lambda}(k+j) \end{bmatrix} = \begin{bmatrix} \mathbf{A} & \mathbf{0} \\ \mathbf{C}^T \mathbf{Q} \mathbf{C} & \mathbf{A}^T \end{bmatrix} \begin{bmatrix} \mathbf{x}(k+j) \\ \boldsymbol{\lambda}(k+j+1) \end{bmatrix} + \begin{bmatrix} \mathbf{0} \\ -\mathbf{C}^T \mathbf{Q} \end{bmatrix} r(k+j) \quad \text{for } j=M, \Lambda, N-1. \quad (20)$$

This version of the control law cannot be implemented in practice, since the boundary conditions are split between times $j=0$ for $\mathbf{x}(k+j)$ and $j=N$ for $\boldsymbol{\lambda}(k+j)$. From Eq. (17), it seems reasonable to assume that for all $j \leq N$, we can write

$$\boldsymbol{\lambda}(k+j) = \mathbf{F}(j)\mathbf{x}(k+j) - \mathbf{g}(k+j). \quad (21)$$

This will turn out to be a valid assumption if consistent equations can be found for $\mathbf{F}(j)$ and $\mathbf{g}(k+j)$. We can solve the following control input through very lengthy derivation:

$$\Delta u_{uv}(k+j) = -\mathbf{K}(j)\mathbf{x}(k+j) + \mathbf{K}_g(j)\mathbf{g}(k+j+1), \quad j=0, 1, \Lambda, M-1, \quad (22)$$

where

$$\mathbf{K}(j) = [\mu + \mathbf{B}^T \mathbf{F}(j+1)\mathbf{B}]^{-1} \mathbf{B}^T \mathbf{F}(j+1)\mathbf{A},$$

$$\mathbf{K}_g(j) = [\mu + \mathbf{B}^T \mathbf{F}(j+1)\mathbf{B}]^{-1} \mathbf{B}^T,$$

$$\mathbf{F}(j) = \mathbf{A}^T \mathbf{F}(j+1) \mathbf{A} - \mathbf{A}^T \mathbf{F}(j+1) \mathbf{B} [\mu + \mathbf{B}^T \mathbf{F}(j+1) \mathbf{B}]^{-1} \mathbf{B}^T \mathbf{F}(j+1) \mathbf{A} + \mathbf{C}^T \mathbf{Q} \mathbf{C},$$

$$\mathbf{F}(N) = \mathbf{C}^T \mathbf{Q}_F \mathbf{C},$$

$$\mathbf{g}(k+j) = \begin{cases} [\mathbf{A} - \mathbf{B} \mathbf{K}(j)]^T \mathbf{g}(k+j+1) + \mathbf{C}^T \mathbf{Q} r(k+j) & \text{for } j \leq M-1 \\ \mathbf{A}^T \mathbf{g}(k+j+1) + \mathbf{C}^T \mathbf{Q} r(k+j) & \text{for } M \leq j \leq N-1 \end{cases}$$

$$\mathbf{g}(k+N) = \mathbf{C}^T \mathbf{Q}_F r(k+N).$$

Since only the first control input is implemented, the control input of the receding horizon controller is as follows:

$$\Delta u_{uv}(k) = -\mathbf{K}(0) \mathbf{x}(k) + \mathbf{K}_g(0) \mathbf{g}(k+1). \quad (23)$$

Therefore, the control input (feedwater flowrate) is calculated as follows:

$$u(k) = v(k) + u(k-1) - v(k-1) - \mathbf{K}(0) \mathbf{x}(k) + \mathbf{K}_g(0) \mathbf{g}(k+1). \quad (24)$$

In Eqs. (23) and (24), $\mathbf{K}(0)$ and $\mathbf{K}_g(0)$ are constants for time-invariant systems. However, $\mathbf{g}(k+1)$ should be solved every time step since the value depends on the reference input (water level setpoint). Since the state $\mathbf{x}(k)$ in Eq. (24) is not measured variables and not exactly known because of modeling inaccuracies, disturbances and noises, in this work, a well-known Kalman filter function of MATLAB [18] is used to observe the state. Figure 3 shows the structure of the designed receding horizon controller. In this figure, it is shown that the changes of the water level setpoint and steam flowrate drive the control actions.

In order to guarantee the closed-loop stability for the proposed controller, the following condition of the matrix inequality must be subjected on the terminal weighting matrix \mathbf{Q}_F [14]:

$$\mathbf{C}^T \mathbf{Q}_F \mathbf{C} \geq \mathbf{A}^T \mathbf{C}^T \mathbf{Q}_F \mathbf{C} (\mathbf{I} + \mathbf{B} \mu^{-1} \mathbf{B}^T \mathbf{C}^T \mathbf{Q}_F \mathbf{C})^{-1} \mathbf{A} + \mathbf{C}^T \mathbf{Q} \mathbf{C}. \quad (25)$$

3. Application to the Steam Generator Water Level Control

The steam generator system is a relatively slow system. Therefore, in numerical simulations, the sampling time was chosen to be 5 sec as recommended in the literature [19] for a liquid level control system. Although most nuclear power plants are usually operated at 100 percent power level (base load), sometimes at startup time and trivial problem occurrences, nuclear power plants can be operated at relatively low power levels. Therefore, in this paper, the steam generator water level controller was designed to deal with these transients (water level deviation and steam flow disturbance) and especially, computer simulations were conducted to investigate the output tracking performance and swell and shrink characteristics. Therefore, it is supposed that the controlled plant was initially in a steady state condition, then the setpoint of the water level increases by step at 500 sec, and the steam flowrate (measurable disturbance) increases by step at 3000 sec and gradually decreases from 5000 sec to 7000 sec.

Note that the steam generator water level process system varies according to the power level but the 2nd order controller design model is fixed within a certain power range. Of course, the receding horizon controller is redesigned automatically if the operating condition of the steam generator is beyond a specified power range. The prediction and control horizons were chosen as 100 and 5, respectively, and the same values were used regardless of power level.

3.1 Linear Model A

Numerical simulations were performed to study the performance of the proposed algorithm. The linear steam generator model described in Eq. (1) was used. The parameter values of a steam generator at several power levels are given in Table 1. Since the parameter values are given at several specific power levels and very different according to the power levels, the parameters of the controlled plant were used by being interpolated versus power. Since $(G_2 - G_1 \tau_2)$ is greater than zero, Eq. (1) has a positive zero that represents a non-minimum phase effect. An unstable zero lowers the control gain to preserve stability. As the load decreases, the zero moves to the right, stability being more critical and the water level of the steam generator being more difficult to control. The transfer function of the design model used to design the receding horizon controller consists of the first and second terms of Eq. (1) as follows:

$$Y(s) = \frac{G_1}{s} [U(s) - V(s)] - \frac{G_2}{1 + \tau_2 s} [U(s) - V(s)]. \quad (26)$$

A controlled plant and a controller design model for numerical simulations are summarized in Table 1. The controller design model in Table 1 was represented by a transfer function with parameter values, G_1 , G_2 and τ_2 . These parameters are a little different from those used in the controlled plant to examine the effects that the parameters are not usually well known. Also, note that we can check the effects of unmodeled dynamics (for example, mechanical oscillation term in Eq. (1)) since the mechanical oscillation term of the controlled plant were not contained in the controller design model. A discrete state equation can be derived from the transfer function of the controller design model to design the proposed controller.

The weighting factors, Q , Q_F and μ are 0.1, 1, and 500000, respectively, which were chosen to meet the stability condition, Eq. (25) and to accomplish good performance. And the same weighting factors were used irrespective of the power level. In these simulations of the linear model *A*, the proposed controller at each power level was designed using the controller design model with the corresponding parameters of each power range.

Figures 4 and 5 show the performances of this proposed controller. In these figures, all values represent the difference from the corresponding steady state values. Therefore, all values are zeros at the steady state. The magnitude of the disturbance at 3000 sec corresponds to 5 percent steam flowrate increase at each power level. The proposed control algorithm tracks well the setpoint and steam flowrate changes. The swell and shrink phenomena are larger at low power levels than those at high power levels. Also, the measured water level tracks its setpoint faster at high powers than at low powers.

Figure 6 shows the performances of the proposed controller and the conventional PI (proportional integral) controller around 5 percent power level. In this simulation, the PI controller gains were optimized by a genetic algorithm (refer to [20]) and also, the several parameters of the proposed controller were changed by focusing on its performance: $N = 54$, $M = 1$, $Q = 1$, $Q_F = 1$ and $\mu = 30000$. The proposed controller shows better performance under steam flowrate disturbances and the step change of the water level setpoint, and also shows a little faster responses.

3.2 Linear Model *B*

Numerical simulations for another linear model were conducted and the linear model is described in Table 2 [15]. The model had been derived by using the thermal hydraulic model of an 857 MWt Westinghouse F-type steam generator [21,22]. The steam generator water level is related with four inputs which are feedwater flowrate, steam flowrate, feedwater temperature, and primary coolant temperature. However, in this work, the effects of feedwater temperature and primary coolant temperature were neglected, which is because their effects are relatively small.

The weighting factors, Q , Q_F and μ are 0.1, 1, and 0.7, respectively and the same weighting factors were used irrespective of the power level. In these simulations of the linear model *B*, the proposed controller at all the power levels is designed by using the controller design model (refer to Table 1) of 100 percent power level. The parameters G_1 and G_2 of the controller design model are corrected so that the units of the linear models *A* and *B* are consistent each other (e.g., rated flowrate and water level unit).

Figures 7 and 8 show the performances of this proposed controller. The simulation situations are the same as those of the linear model *A*. The proposed control algorithm tracks well the setpoint and steam flowrate changes. The swell and shrink phenomena are larger at low power levels than those at high power levels. The measured water level tracks its setpoint faster at high powers than at low powers. The water level transients of the linear model *B* for the steam flowrate disturbance are relatively larger than that of the linear model *A*, which is because that the swell and shrink phenomena due to the steam flowrate change for the linear model *B* are described to be larger than those for the linear model *A*. In these simulations of the linear model *B*, we can see that the swell and shrink phenomena due to the feedwater flowrate change are not described adequately by observing the water level response around 500 sec when the water level setpoint changes suddenly and the feedwater flowrate increases heavily. However, it can be seen that the swell and shrink phenomena due to the steam flowrate change are described well by observing the water level response around 3000 sec when the steam flowrate disturbance occurs.

3.3 Nonlinear Model

The steam generator is actually a nonlinear system. Therefore, the proposed controller has to be verified through implementation on a nonlinear model of the nuclear steam generator to examine its actual performance. The nonlinear model developed by Lee and No [16] was used in this work and Table 2 shows the design

parameters of a steam generator used to develop the nonlinear model. Since the computer code for the nonlinear model is written in the Fortran language, in order to perform the numerical simulations, the proposed control algorithm written in the MATLAB language [18] was interfaced with the code written in the Fortran language.

The weighting factors, Q , Q_F and μ were chosen as 0.5, 1, and 500, respectively. In these simulations of the nonlinear case, the same weighting factors were used irrespective of the power level.

Since this nonlinear model is inadequate to design the controller, the linear model mentioned above (the controller design model at 100 percent power level, refer to Table 1) was used to design the controller. Note that the same controller design model for simulations of all power levels was used. The parameters G_1 and G_2 of the controller design model are corrected so that the units of the linear models A and B are consistent each other. Figures 9 and 10 show the performance of the proposed algorithm for this nonlinear controlled plant. The conditions for the computer simulations of the nonlinear case are the same as those for the linear cases. In the same way as the linear model B , we can see that the swell and shrink phenomena due to the feedwater flowrate change are not described adequately by observing the water level response around 500 sec when the water level setpoint changes suddenly and the feedwater flowrate increases heavily. However, it can be seen that the swell and shrink phenomena due to the steam flowrate change are described well by observing the water level response around 3000 sec when the steam flowrate disturbance occurs. Also, it can be seen that these swell and shrink phenomena are much larger at low powers. Sudden steam disturbance (steam flowrate increase) at 3000 sec induces large surge ranging from about 65 cm to 10 cm for a short time period at 5 percent power simulation. Although the controller design model (refer to Table 1) at 100 percent power (irrespective of actual power levels at the nonlinear controlled plant) was used in designing the proposed algorithm to be implemented on the nonlinear model, its performance is good.

4. Conclusions

In this work, the receding horizon control method was developed to control the water level of nuclear steam generators. The developed controller was applied to the linear and nonlinear models for nuclear steam generators. The steam generator water level controller was designed to effectively deal with water level deviation and steam flow disturbance and especially, computer simulations were conducted to investigate the output tracking performance and swell and shrink characteristics. The parameters of the linear model for a steam generator are very different according to the power levels. However, although the receding horizon controller was designed by using the linear steam generator model fixed over a certain power range, the proposed controller showed good performance for any other power level within the power range. The proposed controller was compared to the PI controller and was known to have better performance. Since the steam generator has nonlinear characteristics, the proposed algorithm was applied to a nonlinear model of the nuclear steam generator to examine its actual performance. Also, the proposed controller showed good performance for the water level setpoint and steam flowrate (measurable disturbance) changes.

Acknowledgment

This work has been conducted under a Korean Nuclear Energy Research Initiative (K-NERI) project supported by the Korea Institute of Science & Technology Evaluation and Planning (KISTEP) which is funded by Korea Ministry of Science and Technology (Korea MOST).

References

1. E. Irving, C. Miossec, and J. Tassart, "Toward Efficient Full Automatic Operation of the PWR Steam Generator with Water Level Adaptive Control," *BNES, London, Boiler Dynamic and Control in Nuclear Power Stations*, pp. 309-329 (1980).
2. M. G. Na and H. C. No, "Design of an Adaptive Observer-Based Controller for the Water Level of Steam Generators," *Nucl. Eng. and Des.*, **135**, 379 (1992).
3. J. J. Feely, *Optimal Digital Estimation and Control of a Natural Circulation Steam Generator*, EG&G Idaho Falls, ID (1981).
4. Y. J. Lee, 1994. "Optimal Design of the Nuclear S/G Digital Water Level Control System," *J. of KNS*, **26**, 32 (1994).
5. C. C. Kuan, C. Lin, and C. C. Hsu, "Fuzzy Logic Control of Steam Generator Water Level in Pressurized Water Reactors," *Nuclear Technology*, **100**, 125 (1992).

6. G. Y. Park and P. H. Seong, "Application of a Fuzzy Learning Algorithm to Nuclear Steam Generator Level Control," *Annals of Nuclear Energy*, **22**, 135 (1995).
7. B. H. Cho and H. C. No, "Design of Stability-Guaranteed Fuzzy Logic Controller for Nuclear Steam Generators," *IEEE Trans. Nucl. Sci.*, **43**, 716 (1996).
8. M. G. Na, "Design of a Genetic-Fuzzy Controller for the Nuclear Steam Generator Water Level Control," *IEEE Trans. Nucl. Sci.*, **45**, 2261 (1998).
9. W. H. Kwon and A. E. Pearson, "A Modified Quadratic Cost Problem and Feedback Stabilization of a Linear System," *IEEE Trans. Automatic Control*, **22**, 838 (1977).
10. J. Richalet, A. Rault, J. L. Testud, and J. Papon, "Model Predictive Heuristic Control: Applications to Industrial Processes," *Automatica*, **14**, 413 (1978).
11. C. E. Garcia, D. M. Prett, and M. Morari, "Model Predictive Control: Theory and Practice – a Survey," *Automatica*, **25**, 335 (1989).
12. M. V. Kothare, V. Balakrishnan, and M. Morari, "Robust Constrained Model Predictive Control Using Linear Matrix Inequality," *Automatica*, **32**, 1361 (1996).
13. J. W. Lee, W. H. Kwon and J. H. Lee, "Receding Horizon H^∞ Tracking Control for Time-Varying Discrete Linear Systems," *Int. J. Control*, **68**, 385 (1997).
14. J. W. Lee, W. H. Kwon, and J. Choi, "On stability of Constrained Receding Horizon Control with Finite Terminal Weighting Matrix," *Automatica*, **34**, 1607 (1998).
15. Y. J. Lee, "Water Level Control of Nuclear Plant Steam Generator," *Trans. on KSME Intl. J.*, **16**, 753 (1992).
16. J. Y. Lee and H. C. No, "Dynamic Scaling Method for Testing the Performance of the Water Level Controller of Nuclear Steam Generators," *Nucl. Eng. Des.* **122**, 313 (1990).
17. M. G. Na and H. C. No, "Quantitative evaluation of swelling or shrinking level contributions in steam generators using spectrum analysis," *Ann. Nucl. Energy*, **20**, 659 (1993).
18. *MATLAB 5.3 (Release 11)*, The MathWorks, Natick, Massachusetts (1999).
19. K. Ogata, *Discrete Time Control Systems*, p. 207, Prentice Hall (1987).
20. M. G. Na, "Design of a Genetic Fuzzy Controller for the Nuclear Steam Generator Water Level Control," *IEEE Trans. Nucl. Sci.*, **45**, 2261 (1998).
21. W. H. Stromayor, *Dynamic Modeling of Vertical U-Tube Steam Generator for Operational Safety Systems*, Ph.D. Thesis, MIT (1982).
22. J. I. Choi, *Non-Linear Digital Control for Steam Generator System in PWR*, Ph.D. Thesis, MIT (1987).

Table 1. Parameters of a steam generator linear model A at several powers.

Controlled plant	$Y(s) = \frac{G_1}{s} [U(s) - V(s)] - \frac{G_2}{1 + \tau_2 s} [U(s) - V(s)] + \frac{G_3 s}{\tau_1^{-2} + 4\pi^2 T^{-2} + 2\tau_1^{-1} s + s^2} U(s)$							
	Power level (%)	G_1	G_2	G_3	τ_1 (sec)	τ_2 (sec)	T (sec)	V_0 (kg/sec)
	5	0.058	9.630	0.181	41.9	48.4	119.6	57.4
	15	0.058	4.46	0.226	26.3	21.5	60.5	180.8
	30	0.058	1.83	0.310	43.4	4.5	17.7	381.7
	50	0.058	1.05	0.215	34.8	3.6	14.2	660.0
	100	0.058	0.47	0.105	28.6	3.4	11.7	1435.0
Controller design model	$Y(s) = \frac{G_1}{s} [U(s) - V(s)] - \frac{G_2}{1 + \tau_2 s} [U(s) - V(s)]$							
	Power level (%)	G_1	G_2	τ_2 (sec)	V_0 (kg/sec)			
	5	0.06	10.0	50.0	57.4			
	15	0.06	5.0	20.0	180.8			
	30	0.06	2.0	5.0	381.7			
	50	0.06	1.0	4.0	660.0			
100	0.06	0.5	4.0	1435.0				

Table 2. Steam generator open loop transfer functions between various inputs and water level (linear model B).

<p>1) Feedwater Flow Rate and Level - $U_1(s, P)$</p> $U_1(s, P) = \frac{1.11 \times 10^{-4}}{s} + K_1(P) \cdot \frac{\omega_n(P)^2}{s^2 + 2\zeta_1(P)\omega_n(P)s + \omega_n(P)^2}$ <p>where,</p> $K_1(P) = -0.01268 e^{-0.0964P} \left(0.04 \left(\frac{P}{5} \right)^2 + 1.16 \right),$ $\zeta_1(P) = 0.2283 e^{0.03P},$ $\omega_n(P) = \frac{\omega_d(P)}{\sqrt{1 - \zeta_1(P)^2}}, \text{ for } \zeta_1 < 1$ $\omega_n(P) = \frac{\omega_d(P)}{\sqrt{\zeta_1(P)^2 - 1}}, \text{ for } \zeta_1 > 1$ $\omega_d(P) = \frac{\pi}{t_p(P)},$ $t_p(P) = 317.7 e^{-0.1764P} + 10$ <p>2) Steam Flow Rate and Level - $U_2(s, P)$</p> $U_2(s, P) = \frac{-1.11 \times 10^{-4}}{s} + K_2(P) \cdot \frac{0.05}{s + 0.05}$ <p>where,</p> $K_2(P) = 0.01957 e^{-0.07348P} + 0.007$ <p>3) Primary Coolant Temp. and Level - $U_3(s, P)$</p> $U_3(s, P) = \left(K_{3,1} \cdot \frac{a-b}{(s+a)(s+b)} - K_{3,2} \cdot \frac{c}{s+c} \right) e^{-2s}$ <p>where,</p> $K_{3,1}(P) = 2.227 \times 10^{-2} + 0.0105P - 6.321 \times 10^{-4} P^2 + 1.17 \times 10^{-5} P^3, \quad P \leq 25\%$ $= 0.071 - 4 \times 10^{-4} \cdot (P - 25), \quad P > 25\%$	$K_{3,2}(P) = 0.004562 + 2.238 \times 10^{-4} P, \quad P \leq 5\%$ $= 0.006186 - 2.634 \times 10^{-4} P + 3.248 \times 10^{-5} P^2, \quad 5\% \leq P \leq 15\%$ $= 0.00042 + 6.082 \times 10^{-4} P, \quad 15\% \leq P \leq 20\%$ $= 0.002752 + 4.916 \times 10^{-4} P, \quad P > 20\%$ $a(P) = 0.084576 + 0.01954P, \quad P \leq 10\%$ $= 0.01725 + 0.01075P, \quad 10\% \leq P \leq 15\%$ $= 0.21 + 0.00825P, \quad 15\% \leq P \leq 20\%$ $= 0.125 + 0.0125P, \quad P > 20\%$ $b(P) = \frac{a(P)}{10}$ $c(P) = 0.001P, \quad P \leq 5\%$ $= -2.0 + 0.04P, \quad 5\% \leq P \leq 10\%$ $= 2.0, \quad P > 10\%$ <p>4) Feedwater Temperature and Level - $U_4(s, P)$</p> $U_4(s, P) = K_4(P) \cdot \frac{\omega_n(P)^2}{s^2 + 2\zeta_4(P)\omega_n(P)s + \omega_n(P)^2}$ <p>where,</p> $K_4(P) = 4.425 \times 10^{-4} e^{0.0348P}, \text{ for all power}$ $\zeta_4(P) = 0.5345 e^{-0.06P}, \quad P \leq 15\%$ $= 0.1716, \quad P > 15\%$ $\omega_n(P) = \frac{\omega_d(P)}{\sqrt{1 - \zeta_4(P)^2}}, \quad \omega_d(P) = \frac{\pi}{t_p(P)}$ $t_p(P) = 195 e^{-0.16P} + 22, \text{ for all power}$
------------------------------------------------------------------------------------------------------------------------------------------------------------------------------------------------------------------------------------------------------------------------------------------------------------------------------------------------------------------------------------------------------------------------------------------------------------------------------------------------------------------------------------------------------------------------------------------------------------------------------------------------------------------------------------------------------------------------------------------------------------------------------------------------------------------------------------------------------------------------------------------------------------------------------------------------------------------------------------------------------------------------------------------------------------------------------------------------------------------------------------------------------------------------------	--------------------------------------------------------------------------------------------------------------------------------------------------------------------------------------------------------------------------------------------------------------------------------------------------------------------------------------------------------------------------------------------------------------------------------------------------------------------------------------------------------------------------------------------------------------------------------------------------------------------------------------------------------------------------------------------------------------------------------------------------------------------------------------------------------------------------------------------------------------------------------------------------------------------------------------------------------------------------------------------------------------------------------------------------------------------------------------------------------------

Table 3. Design parameters of a steam generator used for the nonlinear model (M.K.S. unit).

Name	Size
Cross sectional steam dome area	10.94
Secondary (Primary) heat transfer area	5114 (5114)
Cross sectional tube bundle area	2.699
Cross sectional downcomer area	0.7226
Cross sectional riser inlet area	7.760
Cross sectional riser outlet area	3.243
Downcomer volume	33.21
Steam dome volume	43.15
Boiling region volume	39.79
Riser volume	26.45
Lower downcomer length	10.91
Water level in downcomer	13.17
Parallel flow length in tube	6.960
Tube bundle length	8.460
Riser length	4.640

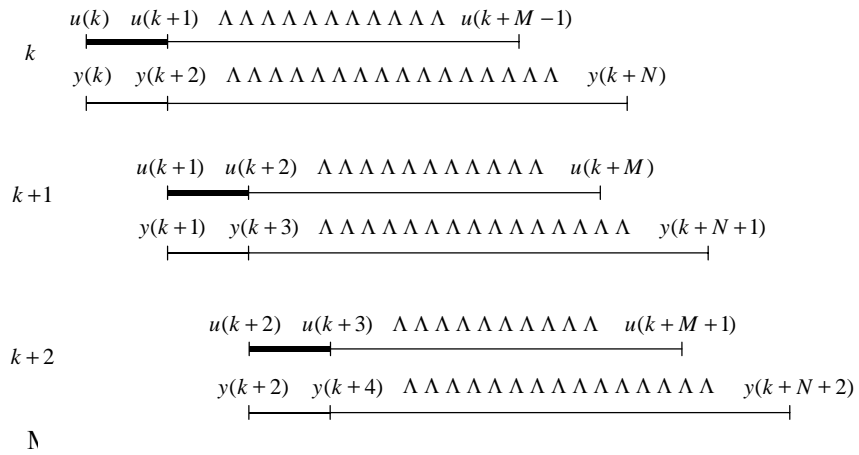


Fig. 1. Optimal solutions and manipulated variables for control implementation.

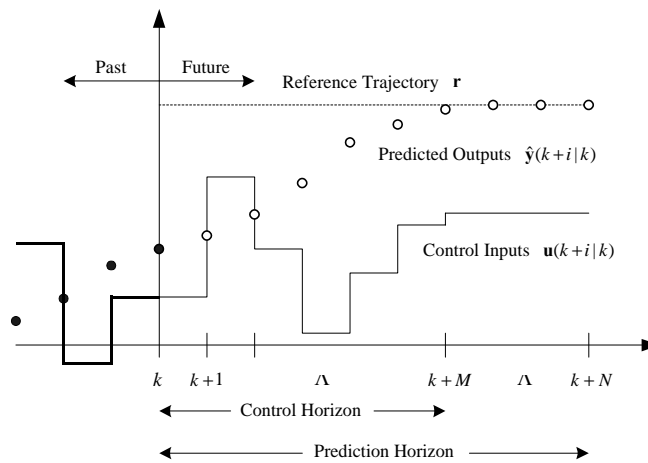


Fig. 2. Basic concept of a receding horizon control method.

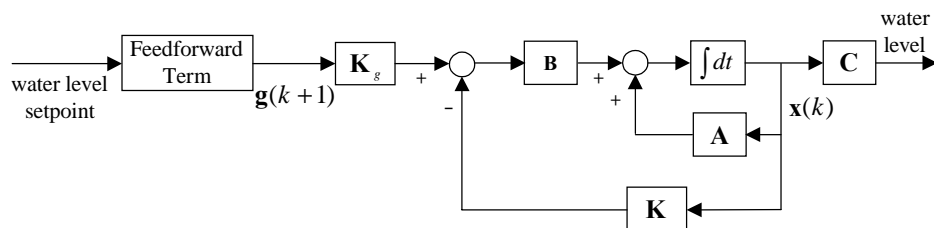
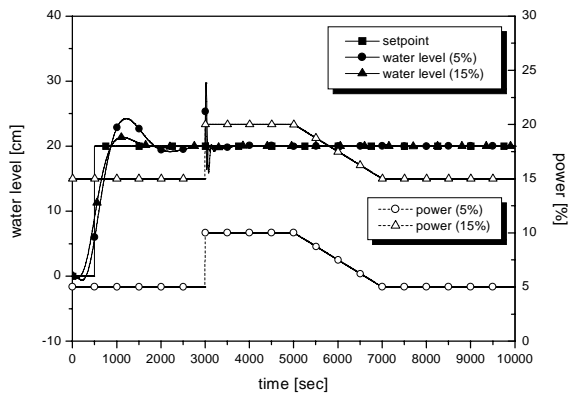
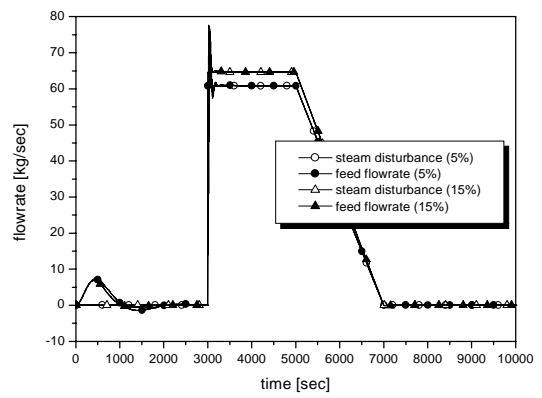


Fig. 3. Block diagram of the designed receding horizon controller.

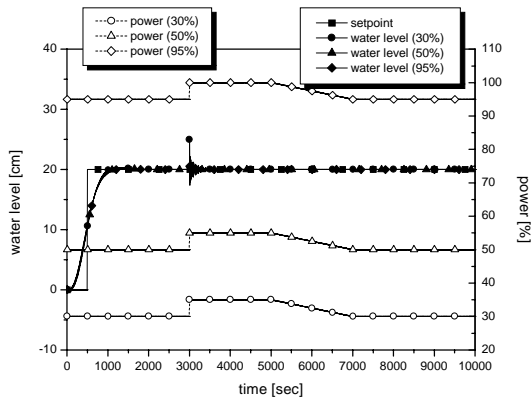


(a) water level

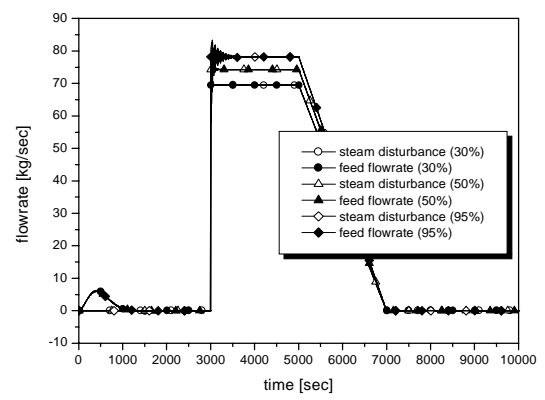


(b) flowrate

Fig. 4. Performance of the proposed controller for the linear model A (low powers).



(a) water level



(b) flowrate

Fig. 5. Performance of the proposed controller for the linear model A (high powers).

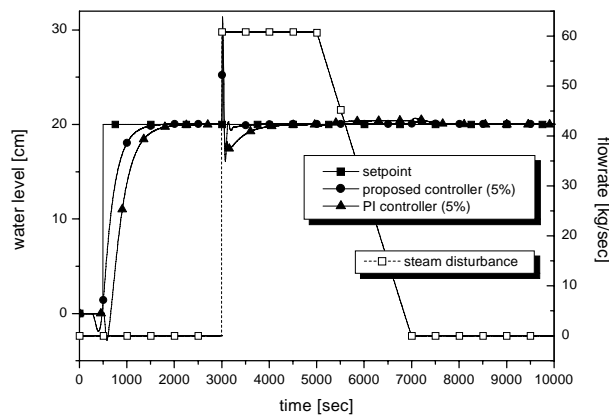
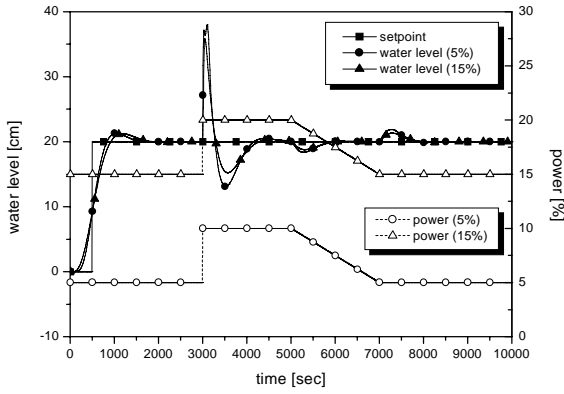
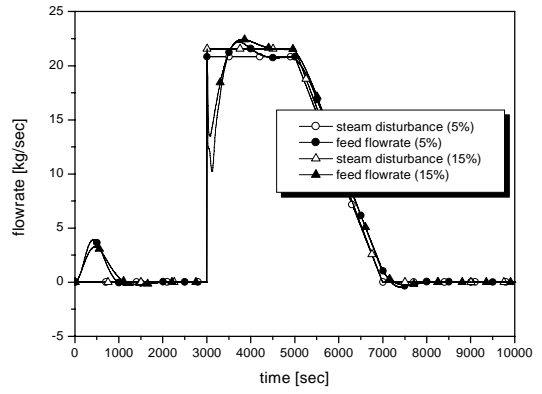


Fig. 6. Comparison of the proposed controller and the PI controller for the linear model A at low power.

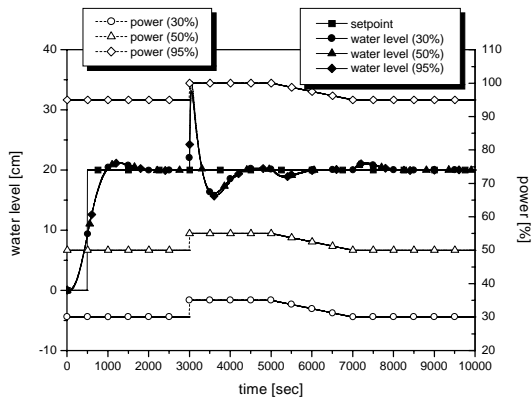


(a) water level

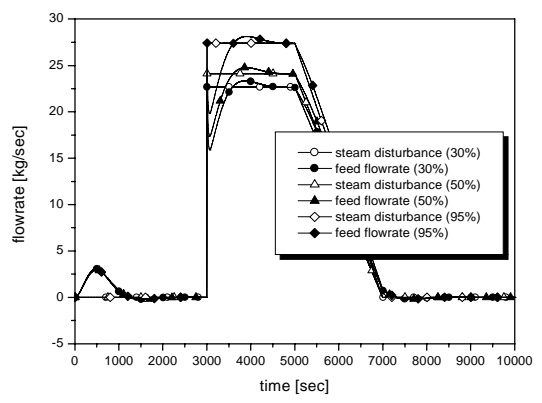


(b) flowrate

Fig. 7. Performance of the proposed controller for the linear model B (low powers).

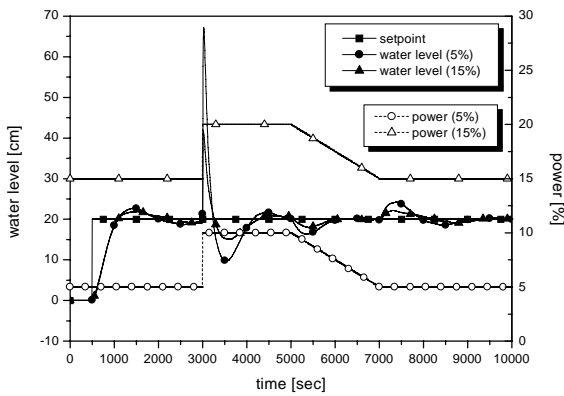


(a) water level

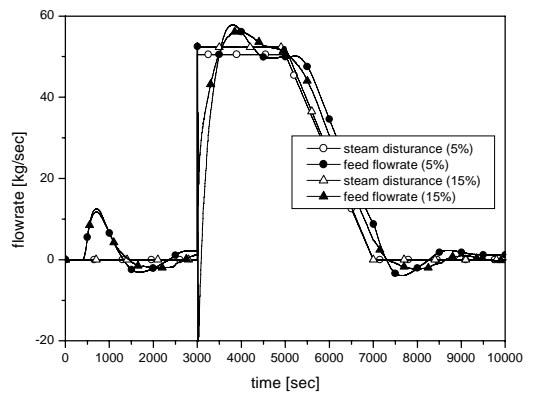


(b) flowrate

Fig. 8. Performance of the proposed controller for the linear model B (high powers).

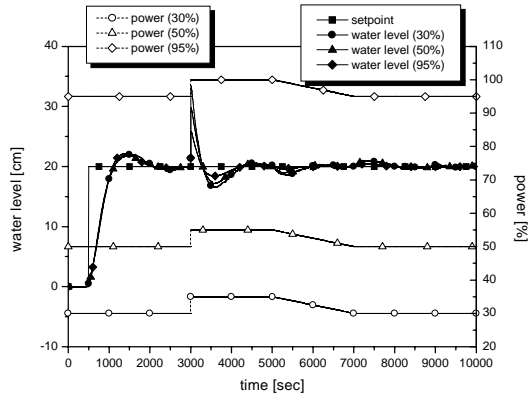


(a) water level

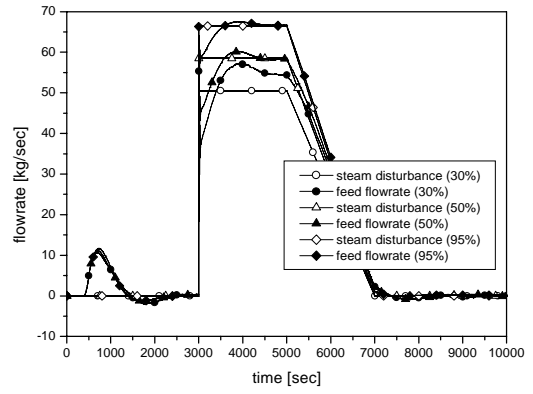


(b) flowrate

Fig. 9. Performance of the proposed controller for the nonlinear model (low powers).



(a) water level



(b) flowrate

Fig. 10. Performance of the proposed controller for the nonlinear model (high powers).